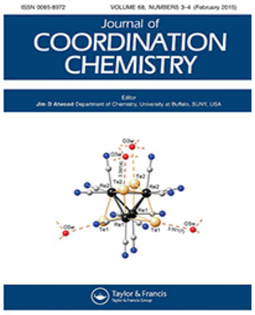

Taylor & Francis
Taylor & Francis Group

Journal of Coordination Chemistry

ISSN: 0095-8972 (Print) 1029-0389 (Online) Journal homepage: http://www.tandfonline.com/loi/gcoo20

Syntheses, structures, magnetic, and luminescent properties of five lanthanide-based MOFs with p-phenylenediamine-tetraacetic acid ligand

Meihui Yu, Xiubo Wang & Ming Hu

To cite this article: Meihui Yu, Xiubo Wang & Ming Hu (2015) Syntheses, structures, magnetic, and luminescent properties of five lanthanide-based MOFs with p-phenylenediamine-tetraacetic acid ligand, Journal of Coordination Chemistry, 68:3, 520-528, DOI: 10.1080/00958972.2014.989842

To link to this article: http://dx.doi.org/10.1080/00958972.2014.989842

Journal of Coordination Chemistry, 2015
Vol. 68, No. 3, 520–528, http://dx.doi.org/10.1080/00958972.2014.989842

Syntheses, structures, magnetic, and luminescent properties of five lanthanide-based MOFs with *p*-phenylenediamine-tetraacetic acid ligand

MEIHUI YU, XIUBO WANG and MING HU*

Inner Mongolia Key Laboratory of Chemistry and Physics of Rare Earth Materials, School of Chemistry and Chemical Engineering, Inner Mongolia University, Hohhot, China

(*Received 25 February 2014; accepted 20 October 2014*)

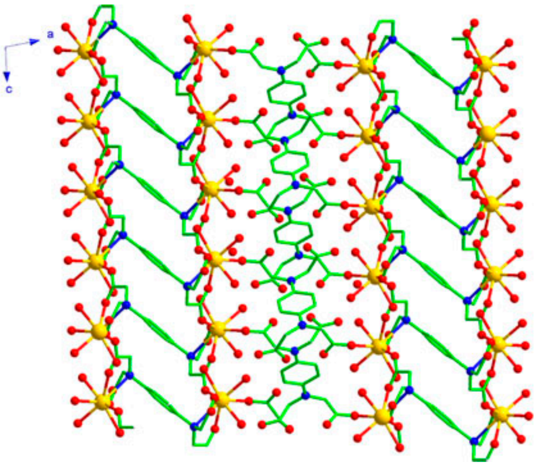

Five lanthanide metal–organic frameworks with *p*-phenylenediamine-tetraacetic acid have been prepared. They are isomorphous and exhibit the 3-D framework structures. The solid-state luminescence of **5** and magnetic property of **4** were investigated.

Five new isomorphous metal–organic frameworks, $\{[Ln(PhDTA)_{0.5}(H_2PhDTA)_{0.5}(H_2O)_3]\cdot H_2O\}_n$ [Ln = Pr (**1**), Sm (**2**), Eu (**3**), Gd (**4**), Tb (**5**)], have been synthesized under solvothermal conditions based on *p*-phenylenediamine-N,N,N′,N′-tetraacetic acid (H_4PhDTA). Compounds **1–5** were characterized by infrared spectra, thermogravimetric analyses and single-crystal X-ray diffraction. Compounds **1–5** crystallize in the monoclinic system with space group of $P2_1/c$ and have 3-D framework structures. The H_2PhDTA^{2-} and H_2PhDTA^{4-} ions exhibit different tetradentate and bidentate modes to connect with lanthanide ions, respectively. The solid-state luminescence of **5** and magnetism of **4** were investigated further.

Keywords: Lanthanide; *p*-Phenylenediamine-N,N,N′,N′-tetraacetic acid; Luminescence; Magnetic property

---

*Corresponding author. Email: hm988@126.com

1. Introduction

The design and fabrication of metal–organic frameworks (MOFs) with desired structures and properties have attracted interest due to their potential applications in gas storage, catalysis, magnetism, fluorescence, etc. [1–12]. Lanthanide coordination compounds usually feature narrow emission peaks as a result of the f–f transitions and may serve as luminescent materials, which are distinct from some compounds of d^{10} transitional metal ions in terms of the dissimilar luminescent mechanism [13–15]. In contrast with transition metal-based MOFs, the design of lanthanide-based MOFs is a challenging task for chemists on account of the versatile coordination environments of lanthanide ions. Diverse lanthanide-based MOFs could be self-assembled because of the disparate coordination geometries and high coordination numbers of the lanthanide ions [16–21]. Lanthanide ions have higher affinity to hard donors, such as carboxylate groups or simultaneously to nitrogen and carboxylate donors in ligands, which are usually employed in the architectures of lanthanide coordination polymers [22–34].

Herein, *p*-phenylenediamine-N,N,N′,N′-tetraacetic acid (H_4PhDTA) is a multicarboxylate ligand containing four nitrogens, which can impart a variety of coordination modes to metal centers and abundant structural motifs. Part of N,N,N′,N′-tetraacetic acid in H_4PhDTA is similar to EDTA, which is a flexible linker and can freely bend and rotate to give peculiar structures when it coordinates with metal centers. In this article, we have prepared five lanthanide coordination polymers by exploiting H_4PhDTA as the starting materials under the solvothermal method, $\{[\mathrm{Ln(PhDTA)_{0.5}(H_2PhDTA)_{0.5}(H_2O)_3}]\cdot\mathrm{H_2O}\}_n$[Ln = Pr (**1**), Sm (**2**), Eu (**3**), Gd (**4**), Tb (**5**)], and their crystal structures, thermal stabilities, luminescence and magnetic properties of some complexes were explored. Some transition metal coordination polymers and a dinuclear gadolinium complex based on H_4PhDTA have been investigated [35, 36], but lanthanide-based MOFs based on H_4PhDTA have not been reported.

2. Experimental

2.1. *Materials and general methods*

H_4PhDTA was synthesized according to the literature procedure [36] and all other reagents for the syntheses were of analytical grade and were used as received from commercial sources. Elemental analyses (C, H, and N) were determined on a Perkin Elmer 2400 analyzer. IR spectra were recorded in KBr disks on a Nicolet Avatar-360 spectrometer from 4000 to 400 $\mathrm{cm^{-1}}$. Thermogravimetric analysis (TGA) was performed on a Perkin Elmer TG-7 analyzer heated from 25 to 800 °C under air. Luminescence spectra were measured on a FLS920 spectrophotometer.

2.2. *Synthesis of $\{[\mathrm{Ln(PhDTA)_{0.5}(H_2PhDTA)_{0.5}(H_2O)_3}]\cdot\mathrm{H_2O}\}_n$*

A mixture of $\mathrm{LnCl_3}\cdot n\mathrm{H_2O}$ [0.1 mM, Ln = Pr (**1**, $n = 7$), Sm (**2**, $n = 6$), Eu (**3**, $n = 6$), Gd (**4**, $n = 6$), Tb (**5**, $n = 6$)] and H_4PhDTA (0.0342 g, 0.1 mM) in 15 mL H_2O and 2 mL C_2H_5OH was stirred for 30 min at room temperature and sealed in a 23 mL Teflon-lined stainless-steel vessel, then heated at 90 °C for 48 h and followed by slow cooling to room temperature at a rate of 5 °C $\mathrm{h^{-1}}$. Crystalline products were obtained, isolated by filtration, then washed with H_2O and air-dried. The yields of **1–5** were 61, 58, 57, 54, and 51%, respectively. IR (KBr pellet): for **1**, 3415(s), 1619(s), 1445(m), 1375(s), 1191, 972(m); for **2**, 3414(s), 1616(s), 1405(s), 1230(m), 977(m), 627(m); for **3**, 3414(s), 1616(s), 1404(s), 1291 (m), 977(m), 627(m); for **4**, 3414(s), 1615(s), 1568(s), 1406(s), 976(m), 628(s); for **5**, 3414 (s), 1615(s), 1406(s), 1292(m), 976(m), 629(m). Elemental analysis (%): For **1**, Calcd C 30.53, H 3.82, N 5.09, found: C 30.50, H 3.84, N 5.04; for **2**, Calcd C 30.02, H 3.75, N 5.00, found: C 30.03, H 3.71, N 4.98; for **3**, Calcd C 29.93, H 3.74, N 4.99, found: C 29.90, H 3.75, N 4.97; for **4**, Calcd C 29.65, H 3.71, N 4.94, found: C 29.66, H 3.72, N 4.96; for **5**, Calcd 29.56, H 3.70, N4.93, found: C 29.53, H 3.72, N 4.90.

2.3. *X-ray crystallography*

Crystallographic data for **1–5** were collected on a Bruker ApexII Smart CCD diffractometer with graphite-monochromated Mo-$K\alpha$ radiation ($\lambda = 0.71073$ Å) using the ω-scan technique at room temperature. All structures were solved by direct methods with SHELXS-97 and refined with full-matrix least-squares $|F|^2$ technique using the SHELXL-97 [37, 38] program. The positions of nonhydrogen atoms were refined with anisotropic displacement parameters. The hydrogens were set in calculated positions and refined as riding with a common isotropic thermal parameter. The crystallographic data for **1–5** are listed in table 1; selected bond lengths and angles of **1–5** are listed in tables S1–S5 (see online supplemental material at http://dx.doi.org/10.1080/00958972.2014.989842).

3. Results and discussion

3.1. *Crystal structure of $\{[Ln(PhDTA)_{0.5}(H_2PhDTA)_{0.5}(H_2O)_3]\cdot H_2O\}_n$*

Single-crystal X-ray diffraction analysis reveals that **1–5** are isomorphous structures, which belong to monoclinic system with space group of $P2_1/c$. Therefore, the only structure of **2**

Table 1. The crystallographic data for **1–5**.

Compound	**1**	**2**	**3**	**4**	**5**
Formula	$C_{14}H_{21}PrN_2O_{12}$	$C_{14}H_{21}SmN_2O_{12}$	$C_{14}H_{21}EuN_2O_{12}$	$C_{14}H_{21}GdN_2O_{12}$	$C_{14}H_{21}TbN_2O_{12}$
Formula weight	550.24	559.69	561.30	566.58	568.26
T (K)	296(2)	296(2)	296(2)	296(2)	296(2)
Crystal system	Monoclinic	Monoclinic	Monoclinic	Monoclinic	Monoclinic
Space group	$P2_1/c$	$P2_1/c$	$P2_1/c$	$P2_1/c$	$P2_1/c$
a (Å)	19.2783(18)	19.2745(16)	19.222(4)	19.2827(9)	19.2821(16)
b (Å)	10.1058(9)	10.0836(9)	10.057(2)	10.0611(5)	10.0525(9)
c (Å)	9.7172(9)	9.6577(8)	9.602(2)	9.6227(4)	9.6030(8)
α (°)	90.00	90.00	90.00	90.00	90.00
β (°)	98.884(2)	98.6470(10)	98.620(4)	98.5770(10)	98.527(2)
γ (°)	90.00	90.00	90.00	90.00	90.00
V (A^3)	1870.4(3)	1855.7(3)	1835.3(7)	1845.97(15)	1840.8(3)
Z	4	4	4	4	4
D_{Calcd} (g cm^{-3})	1.954	2.003	2.031	2.039	2.050
μ (mm^{-1})	2.674	3.234	3.488	3.663	3.912
$F(0\,0\,0)$	1096.0	1108.0	1112	1116.0	1120.0
R_{int}	0.0249	0.0190	0.0389	0.0231	0.0260
GOOF	1.042	1.038	1.042	1.046	1.096
R_1[a]	0.0213	0.0199	0.0315	0.0231	0.0359
ωR_2[b] [$I > 2\sigma(I)$]	0.0537	0.0471	0.0764	0.0550	0.0940
R_1 (all data)	0.0275	0.0238	0.0406	0.0308	0.0416
wR_2 (all data)	0.0572	0.0498	0.0815	0.0601	0.0974

[a] $R_1 = \Sigma||F_o| - |F_c||/\Sigma|F_o|$.

[b] $\omega R_2 = [\Sigma[\omega(F_o^2 - F_c^2)^2]/\Sigma\omega(F_o^2)^2]^{1/2}$.

is described. The asymmetric unit of **2** contains one Sm^{3+}, a half independent $PhDTA^{4-}$, a half independent H_2PhDTA^{2-}, three coordinated waters, and one lattice water. The eight-coordinate Sm^{3+} has four monodentate carboxylate oxygens (O4, O5, O6, O8) from two $PhDTA^{4-}$ ligands and one H_2PhDTA^{2-} ligand, N2 from $PhDTA^{4-}$, and three water molecules (O9, O10, O11). The coordination environment of Sm^{3+} can be described as a distorted bicapped trigonal prism, in which O8 and O11 are capping atoms (figure 1). The Sm–O distances are 2.3807(17)–2.4465(16) Å and Sm–N length is 2.828(2) Å. The $PhDTA^{4-}$ and H_2PhDTA^{2-} ions exhibit two coordination modes as shown in scheme 1, acting as a tetradentate and a bidentate linker with lanthanide ions, respectively. As shown in figure 2, the Sm^{3+} ions are connected by carboxylate oxygens to generate a 2-D layer viewed along the *b* axis, in which two coordination modes of ligands alternate. Then, the 2-D planes are further linked by ligands into a 3-D architecture, which is shown in figure 3. In **1–5**, the average bond lengths of Ln–O and Ln–N display a decreasing trend with increase in atomic number from **1**-Pr (2.45 Å) to **5**-Tb (2.37 Å) and **1**-Pr (2.85 Å) to **5**-Tb (2.81 Å).

3.2. *Thermogravimetric analysis*

The thermal analyses of **1–5** were detected with a heating rate of 5 °C min^{-1} from 25 to 800 °C under air, as shown in figure 4. The first weight losses of **1–5** between 100 and 170 °C are 14.47, 11.83, 11.98, 12.69, and 12.88%, respectively, corresponding to loss of three coordination and one lattice water (calc. 13.08% for **1**, 12.86% for **2**, 12.83% for **3**, 12.71% for **4**, and 12.67% for **5**, respectively). The second weight loss from 175 to 260 °C stems from the departure of a CH_2COOH group (obsd. 10.74% for **1**, 10.77% for **2**, 10.57% for **3**, 10.53% for **4**, and 10.25% for **5**, respectively; calc. 10.72% for **1**, 10.54% for **2**, 10.51% for **3**, 10.41% for **4**, and 10.38% for **5**, respectively). The third weight loss from 270 to 360 °C corresponds to removal of $–NCH_2COOH$ (obsd. 13.40% for **1**, 13.73% for **2**, 12.63% for **3**, 13.35% for **4**, and 13.56% for **5**, respectively; calc. 13.26% for **1**, 13.04% for **2**, 13.01% for **3**, 12.88% for **4**, and 12.85% for **5**, respectively). Finally, strong exothermal

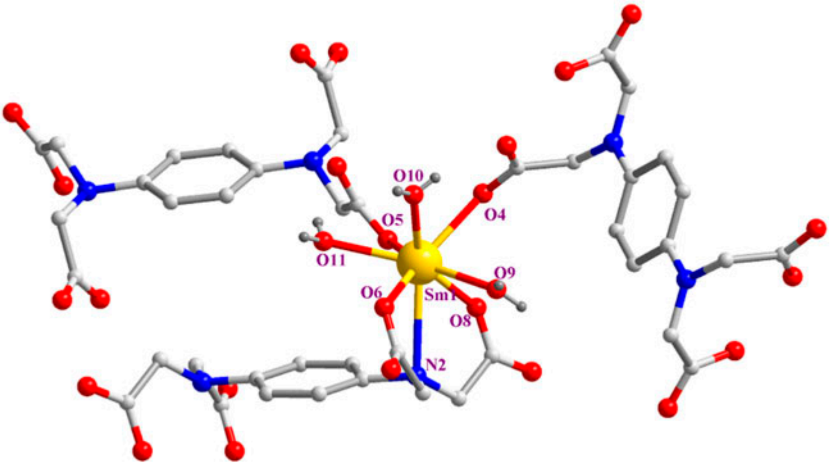

Figure 1. The coordination environment of Sm^{3+} in **2**.

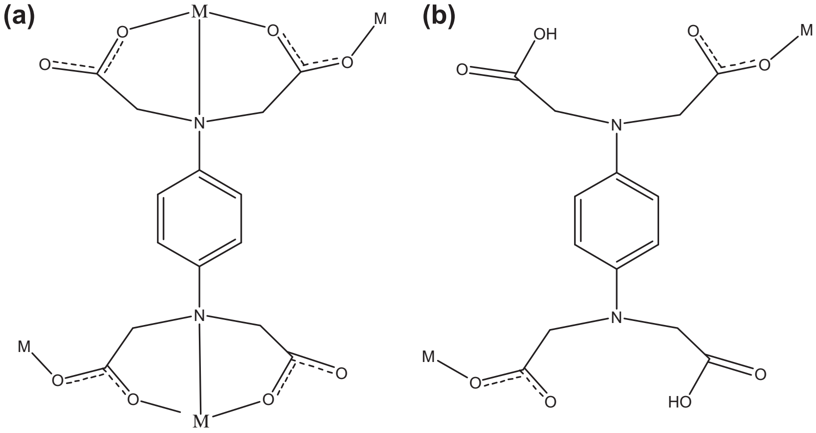

Scheme 1. The coordination modes of (a) $PhDTA^{4-}$ and (b) H_2PhDTA^{2-}.

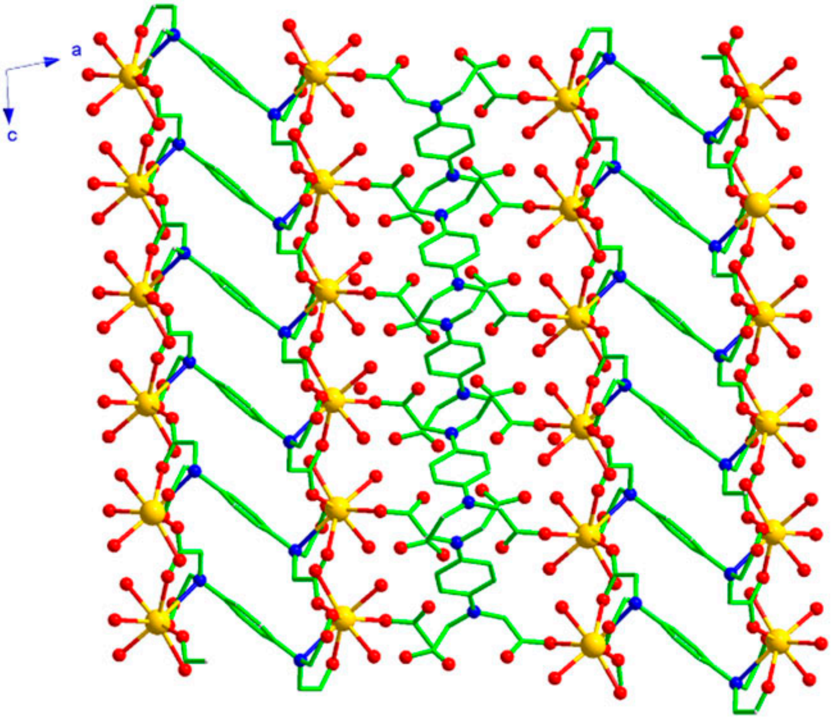

Figure 2. A view of the 2-D sheet along the *b* axis in **2**.

processes for **1–5** begin at 430 °C and suggest decomposition of frameworks. The residues are lanthanide oxides (obsd. 28.82% for **1**, 32.27% for **2**, 32.20% for **3**, 34.03% for **4**, and 31.30% for **5**, respectively; calcd 30.01% for Pr_2O_3, 31.16% for Sm_2O_3, 31.35% for Eu_2O_3, 31.99% for Gd_2O_3, and 32.91% for Tb_4O_7, respectively).

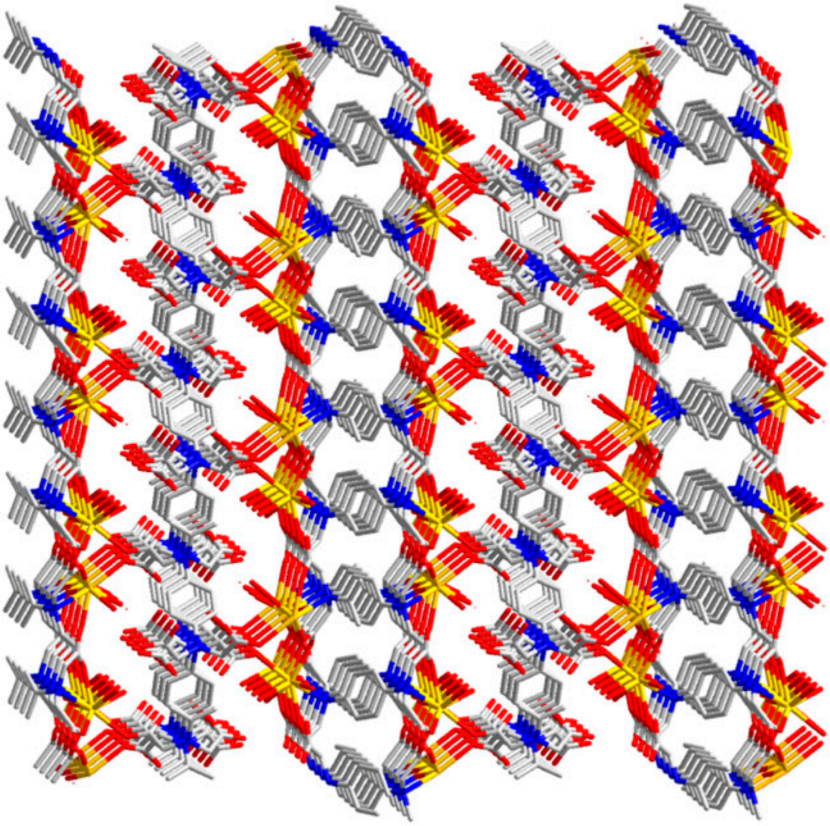

Figure 3. The 3-D framework architecture of **2**.

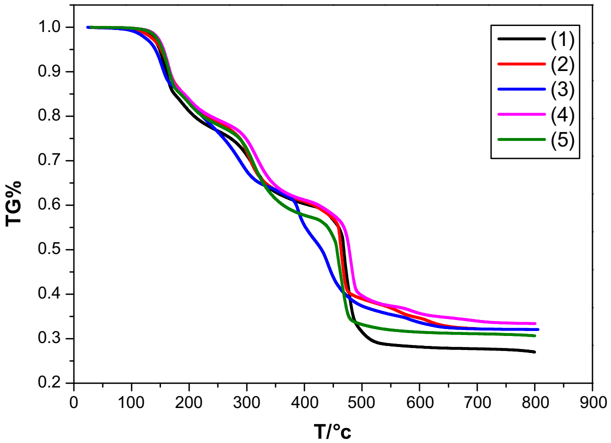

Figure 4. TGA curves of **1–5**.

In order to check the phase purity of **2**, **3**, and **5**, the X-ray powder diffraction (XRPD) patterns were checked at room temperature. As shown in figure 5, most peak positions of simulated and experimental patterns are in agreement with each other. The differences in intensity may be due to the preferred orientation of the crystalline powder samples.

3.3. *Luminescent properties*

The solid-state luminescences of **2**, **3**, and **5** were measured at room temperature. Compounds **2** and **3** do not exhibit the characteristic luminescent emission peaks of lanthanide ions, which may be ascribed to inefficient ligand-to-metal energy transfer [39]. The emission spectrum of **5** is shown in figure 6 ($\lambda_{ex} = 310$ nm); four characteristic peaks of Tb^{3+} are assigned to the $^5D_4 \rightarrow {}^7F_J$ ($J = 6, 5, 4, 3$) transitions, namely, $^5D_4 \rightarrow {}^7F_6$ (488 nm), $^5D_4 \rightarrow {}^7F_5$ (543 nm), $^5D_4 \rightarrow {}^7F_4$ (585 nm), $^5D_4 \rightarrow {}^7F_3$ (620 nm), respectively. The most intense emission peak is the hypersensitive transition $^5D_4 \rightarrow {}^7F_5$ [40], the strong intensity of **5** make it a desired candidate for luminescence-emitting materials.

3.4. *Magnetic property*

Variable-temperature magnetic susceptibility was carried out for **4** from 2 to 300 K at an applied field of 1000 Oe. As shown in figure 7, the experimental $\chi_M T$ value is 7.81 cm^3 K M^{-1} at 300 K, which is close to the calculated value of 7.88 cm^3 K M^{-1} for free Gd(III) on ground level of $^8S_{7/2}$. Upon further cooling, $\chi_M T$ decreases gradually and reaches the minimum value of 6.79 cm^3 K M^{-1} at 2 K. This is suggestive of the presence of antiferromagnetic coupling between Gd(III) ions. Temperature dependence of the reciprocal susceptibility ($1/\chi_M$) obeys the Curie–Weiss law, with the Weiss constant $\theta = -1.71$ K and Curie constant $C = 7.81$ cm^3 K M^{-1}. The small negative Weiss constant indicates weak antiferromagnetic interactions between Gd(III) ions [41, 42].

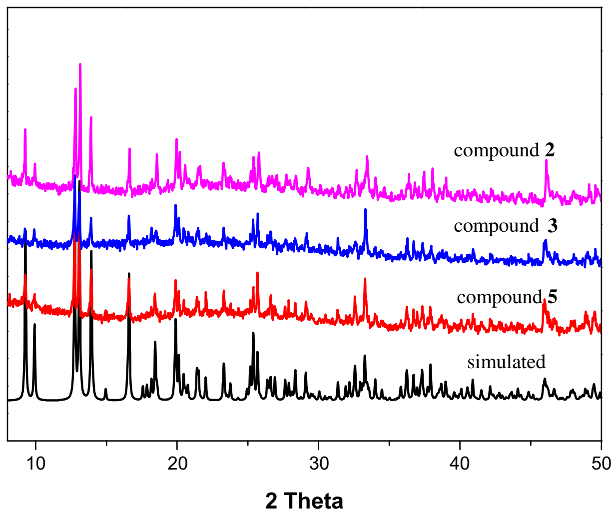

Figure 5. PXRD and simulated patterns of **2**, **3**, and **5**.

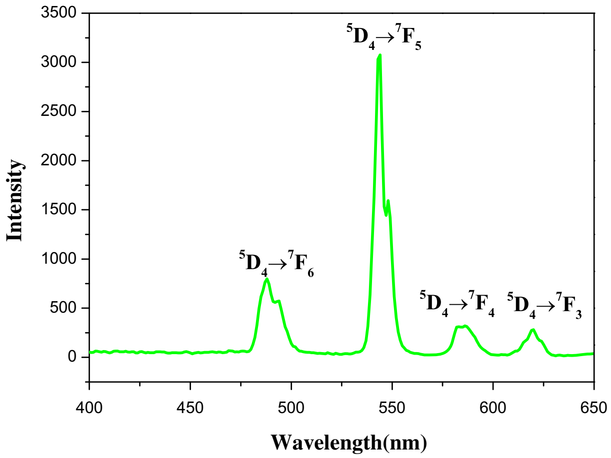

Figure 6. The emission spectrum of **5**.

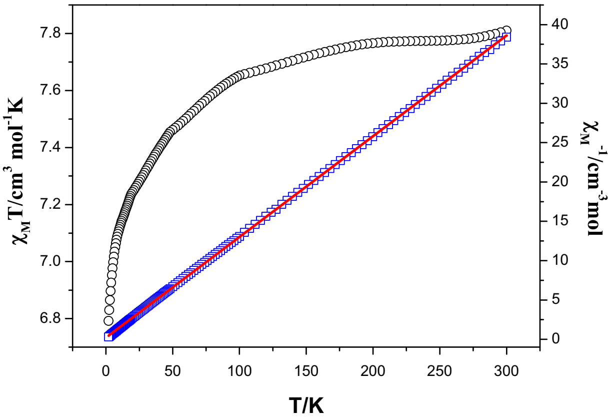

Figure 7. Temperature dependence of $\chi_M T$ and χ_M^{-1} curve of **4**.

4. Conclusion

Five lanthanide MOFs based on *p*-phenylenediamine-tetraacetic acid have been prepared by the solvothermal method. Compounds **1–5** are isomorphous and exhibit 3-D framework structures. The luminescence of **5** displays the characteristic emission peaks of Tb^{3+} ion. Magnetic property of **4** was explored, which indicates the presence of an antiferromagnetic interaction between Gd(III) ions.

Supplementary material

CCDC No. 960464 for **1**, 960465 for **2**, 960466 for **3**, 960467 for **4**, and 960468 for **5** can be obtained from the Cambridge Crystallographic Data Center free of charge via www.ccdc.cam.ac.uk/data_request/cif.

Funding

This work is financially supported by the National Natural Science Foundation of China [grant number 21361017]; Inner Mongolia Natural Science Foundation [grant number 2012MS0214]; the Scientific and Technological Key Research Project of Inner Mongolia Colleges & Universities [grant number NJZZ12012].

References

[1] M. O'Keeffe, O.M. Yaghi. *Chem. Rev.*, **112**, 675 (2012).
[2] P.F. Shi, B. Zhao, G. Xiong, Y.-L. Hou. *Chem. Commun.*, **48**, 8231 (2012).
[3] W.J. Yu, X. Chen, J. Li, B. Li, T.L. Zhang, J. Tao. *CrystEngComm*, **15**, 7732 (2013).
[4] L. Cheng, Q.N. Cao, X.Y. Zhang, S.H. Gou, L. Fang. *J. Coord. Chem.*, **66**, 481 (2013).
[5] P. Thakur, J.L. Conca, G.R. Choppin. *J. Coord. Chem.*, **64**, 3215 (2011).
[6] S. Sharif, O. Sahin, I.U. Khan, O. Büyükgüngör. *J. Coord. Chem.*, **65**, 1892 (2012).
[7] Y.K. He, J. Li, P. Zhang, X. Chen, Y. Ma, Z.B. Han. *J. Coord. Chem.*, **61**, 2876 (2008).
[8] J.M. Zhou, W. Shi, N. Xu, P. Cheng. *Cryst. Growth Des.*, **13**, 1218 (2013).
[9] Q. Gao, C.Y. Zhang, W.H. Gao, Y. Wu, Y.B. Xie, J.H. Sun. *J. Coord. Chem.*, **62**, 2689 (2009).
[10] S.Q. Su, W. Chen, C. Qin, S.Y. Song, Z. Guo, G. Li. *Cryst. Growth Des.*, **12**, 1808 (2012).
[11] Z.R. Pan, H.G. Zheng, T.W. Wang, Y. Song, Y.Z. Li, Z.J. Guo, S.R. Batten. *Inorg. Chem.*, **47**, 9528 (2008).
[12] Y.F. Bi, X.T. Wang, B.W. Wang, W.P. Liao, X.F. Wang, H.J. Zhang, S. Gao, D.Q. Li. *Dalton Trans.*, 2250 (2009).
[13] R. Decadt, K. Van Hecke, D. Depla, K. Leus, D. Weinberger, I. Van Driessche, P. Van Der Voort. *Inorg. Chem.*, **51**, 11623 (2012).
[14] T.L. Chen, X.Y. Yu, X. Zhao. *Inorg. Chem. Commun.*, **23**, 74 (2012).
[15] Z.Q. Jiang, G.Y. Jiang, D.C. Hou. *CrystEngComm*, **15**, 315 (2012).
[16] J. Yang, S.Y. Song, J.F. Ma, Y.Y. Liu, Z.T. Yu. *Cryst. Growth Des.*, **11**, 5469 (2011).
[17] X. Wang, Q.G. Zhai, S.N. Li, Y.C. Jiang, M.C. Hu. *Cryst. Growth Des.*, **14**, 177 (2014).
[18] H.L. Guo, Y.Z. Zhu, S.L. Qiu, J.A. Lercher, H.J. Zhang. *Adv. Mater.*, **22**, 4190 (2010).
[19] J. Xu, J. Cheng, W. Su, M. Hong. *Cryst. Growth Des.*, **11**, 2294 (2011).
[20] M.D. Allendorf, C.A. Bauer, R.K. Bhakta, R.J. Houk. *Chem. Soc. Rev.*, **38**, 1330 (2009).
[21] P.F. Shi, Z. Chen, G. Xiong, B. Shen, J.Z. Sun, P. Cheng, B. Zhao. *Cryst. Growth Des.*, **12**, 5203 (2012).
[22] H.L. Gao, L. Yi, B. Zhao, X.Q. Zhao, P. Cheng, D.Z. Liao, S.P. Yan. *Inorg. Chem.*, **45**, 4980 (2006).
[23] X.X. Xu, X.X. Liu, T. Sun, X. Zhang, E.B. Wang. *J. Coord. Chem.*, **62**, 2755 (2009).
[24] B.M. Ji, D.S. Deng, X. He, B. Liu, S.B. Miao, N. Ma, W.Z. Wang, L.G. Ji, P. Liu, X.F. Li. *Inorg. Chem.*, **51**, 2170 (2012).
[25] R. Feng, L. Chen, Q.H. Chen, X.C. Shan, Y.L. Gai, F.L. Jiang, M.C. Hong. *Cryst. Growth Des.*, **11**, 1705 (2011).
[26] H.Y. Liu, Y.J. Yuan, Z.T. Yu, Z.G. Zou. *CrystEngComm*, **13**, 2391 (2011).
[27] K.C. Szeto, K.O. Kongshaug, S. Jakobsen, M. Tilset, K.P. Lillerud. *Dalton Trans.*, **15**, 2054 (2008).
[28] L.R. Yang, S. Song, H.M. Zhang, W. Zhang, L.Z. Wu, Z.W. Bu, T.G. Ren. *Synth. Met.*, **162**, 261 (2012).
[29] C. Butler, S. Goetz, C.M. Fitchett, P.E. Kruger, T. Gunnlaugsson. *Inorg. Chem.*, **50**, 2723 (2011).
[30] H.S. Wang, B. Zhao, B. Zhai, W. Shi, P. Cheng, D.Z. Liao, S.P. Yan. *Cryst. Growth Des.*, **7**, 1851 (2007).
[31] M. Fang, P.F. Shi, B. Zhao, D.X. Jiang, P. Cheng, W. Shi. *Dalton Trans.*, **41**, 6820 (2012).
[32] F.C. Liu, Y.F. Zeng, J.P. Zhao, B.W. Hu, X. Hu, J. Ribas, X.H. Bu. *Dalton Trans.*, 2074 (2009).
[33] N.R. Kelly, S. Goetz, S.R. Batten, P.E. Kruger. *CrystEngComm*, **10**, 1018 (2010).
[34] J.W. Dai, M.L. Tong. *CrystEngComm*, **14**, 2124 (2012).
[35] C.A. González, M. Hernández-Padilla, S. Dominguez, A. Mederos, F. Brito, J.M. Arrieta. *Polyhedron*, **16**, 2925 (1997).
[36] F.Y. Yu, Z.F. Hao, H.F. Li, S. Hu. *Chin. J. Struct. Chem.*, **31**, 1315 (2012).
[37] G.M. Sheldrick. *Acta Crystallogr.*, **64**, 112 (2008).
[38] G.M. Sheldrick. *SHELXL-97 Program for Crystal Structures Refinement*, University of Gottingen, Gottingen (1997).
[39] (a) M. Latva, H. Takalo, V.M. Mukkala, C. Matachescu, J.C. Rodríguez-Ubis, J. Kankare. *J. Lumin.*, **75**, 149 (1997); (b) Y.L. Guo, W. Dou, X.Y. Zhou, W.S. Liu, W.W. Qin, Z.P. Zang, H.R. Zhang, D.Q. Wan. *Inorg. Chem.*, **48**, 3581 (2009); (c) P.R. Matthes, J. Nitsch, A. Kuzmanoski, C. Feldmann, A. Steffen, T.B. Marder, K. Muller-Buschbaum. *Chem. Eur. J.*, **19**, 17369 (2013).
[40] (a) R. Shyni, S. Biju, M.L.P. Reddy, A.H. Cowley, M. Findlater. *Inorg. Chem.*, **46**, 11025 (2007); (b) Y.W. Wang, Y.L. Zhang, W. Dou, A.J. Zhang, W.W. Qin, W.S. Liu. *Dalton Trans.*, **39**, 9013 (2010).
[41] S.T. Hatscher, W. Urland. *Angew. Chem. Int. Ed.*, **42**, 2862 (2003).
[42] M.H. Molina, C.R. Perez, T. Lopez, F. Lloret, M. Julve. *Inorg. Chem.*, **42**, 5457 (2003).